Plant Biotechnology Journal

WILEY

RESEARCH ARTICLE OPEN ACCESS

Phage Display Derived Antibodies Against Antimicrobial Peptide *Fs*PDF2 Reveal Stress Response in European Beech

Philip Alexander Heine[1,2] | Tetyana Nosenko[3] | Sarah Kistner[4] | Kevin Dennis Oliphant[4] | Manuel Hanke-Uhe[5] | Afsheen Shahid[6] | Bin Hu[7] | Martin Kucklick[8,9] | Nina Lehmler[1] | Marlies Becker[1] | Nicole Goerke[4] | Janin Korn[1] | Tanja Linke[4] | Doris Meier[1] | Asta Perl[4] | Saskia Polten[1,2] | Valeska Priess[1] | Dorina Schäckermann[1,10] | Maren Schubert[1] | Jörg Schumacher[5] | Jana Barbro Winkler[3] | Susanne Engelmann[8,9] | Heinz Rennenberg[6,7] | Jörg-Peter Schnitzler[3] | Stefan Dübel[1] | Michael Hust[1,2] | Robert Hänsch[4,7,11] | David Kaufholdt[4]

[1]Department of Biotechnology, Technische Universität Braunschweig, Braunschweig, Germany | [2]Department of Medical Biotechnology, Technische Universität Braunschweig, Braunschweig, Germany | [3]Research Unit Environmental Simulation (EUS), Helmholtz Zentrum München, Neuherberg, Germany | [4]Institute of Plant Biology, Technische Universität Braunschweig, Braunschweig, Germany | [5]Faculty for Forest and Environment, Eberswalde University for Sustainable Development, Eberswalde, Germany | [6]Institute of Forest Sciences, Chair of Tree Physiology, Albert-Ludwigs-University Freiburg, Freiburg, Germany | [7]Center of Molecular Ecophysiology (CMEP), College of Resources and Environment, Southwest University, Chongqing, P. R. China | [8]Institute for Microbiology, Technische Universität Braunschweig, Braunschweig, Germany | [9]Helmholtz Center for Infection Research, Microbial Proteomics, Braunschweig, Germany | [10]Wirtschaftsgenossenschaft deutscher Tierärzte eG (WDT), Garbsen, Germany | [11]Department of Biosciences and Bioengineering, Indian Institute of Technology, Roorkee, Uttarakhand, India

Correspondence: Robert Hänsch (r.haensch@tu-braunschweig.de)

Received: 3 September 2024 | **Revised:** 9 May 2025 | **Accepted:** 13 October 2025

Funding: This study was financially supported by the Waldklimafond (WKF) via the Fachagentur für Nachwachsende Rohstoffe e.V. (FNR) commissioned by the German Federal Ministry of Food and Agriculture (BMEL) and the Federal Ministry for the Environment, Nature Conservation, Nuclear Safety and Consumer Protection (BMUV) (grant 28W-B-4-130-01) to R.H., H.R., J.-P.S. and J.S. as well as by the Deutsche Forschungsgemeinschaft (INST 188/365-1 FUGG DFG) to S.E.

Keywords: AMP quantification | antimicrobial peptides | crude plant extract ELISA | drought/biotic stress | forest stress diagnostic | phage display recombinant antibodies | plant defensins

ABSTRACT

Plant defensins (PDFs) are cysteine-rich antimicrobial peptides (AMPs) that are important components of plant immunity. They occur constitutively in various plant tissues but are also upregulated upon stress. Therefore, these molecules are of great interest as markers for the diagnosis of early forest stress response in plants at the molecular level. PDFs are small peptides (~5 kDa) with a compact tertiary structure, requiring specific protocols and dedicated antibodies for detection by quantitative ELISA. We developed monoclonal recombinant antibodies using phage display in solution against the correctly folded antigen defensin *Fs*PDF2 from beech (*Fagus sylvatica*) and analysed the antibody–antigen interaction in silico with AlphaFold 3. In a proof-of-principle study, we investigated the *Fs*PDF2 stress response to abiotic (drought) and biotic (gall midge) stresses. Notably, we established an assay for defensin quantification in crude plant extract, detecting for the first time natively folded proteins in a specific sandwich ELISA. Our antibody generation strategy can be transferred by practitioners to other small antimicrobial peptides (AMP), paving the way to study this group of proteins and their corresponding stress response comprehensively.

1 | Introduction

Plants have to cope with a wide range of abiotic and biotic stressors in their environment, such as drought, flooding, herbivory and pathogens. As sessile organisms, plants cannot escape from stress exposure, but rather must develop a more effective immune system. Forest ecosystems are especially suffering from global climate change, triggering an increasing frequency, duration and intensity of extreme weather events (Dyderski et al. 2018) that also enhance the virulence of (invasive) plant pathogens (Stenlid and Oliva 2016).

Antimicrobial peptides (AMPs) are important components of the eukaryotic innate immune system toolbox. In plants, AMPs induce resistance to pathogens and tolerance to abiotic stresses (dos Santos-Silva et al. 2020). Due to their antimicrobial and immunomodulatory activities against infectious bacteria (Gram-positive and Gram-negative), AMPs have received increasing interest as potential agents for developing drugs against human pathogens in recent years (Lazzaro et al. 2020; Srivastava et al. 2021). Plant defensins (PDF) are essential members within the large group of AMPs; they were first described in wheat and barley seedlings (Méndez et al. 1996). At 48–54 amino acids, these proteins have a relatively low molecular weight (5 kDa) with a tertiary structure defined by an α-helix and three antiparallel β-sheets. Four disulfide bonds that form a CSαβ motif stabilize the structure (De Coninck et al. 2013). Defensins also possess a γ-core motif GXC(X3-9)C, which is conserved in disulfide-containing peptides and leads to a stable globular structure (Yount and Yeaman 2004).

Many PDFs with multiple modes of action against different stressors have been identified throughout the plant kingdom (van der Weerden and Anderson 2013). In *Arabidopsis thaliana*, 15 PDFs and 320 defensin-like peptides have been described Arputharaj (2017). Their primary amino acid sequence can vary widely. However, the CSαβ motif in the secondary structure and the four cysteine bridges in the tertiary structure are highly conserved domains. PDFs and defensin-like peptides mainly occur in the apoplastic space of all plant organs such as leaves, roots, wood, flowers and seeds as well as in almost all tissues including xylem, bark, stamens, pollen and leaf stomata or parenchyma (de Oliveira Carvalho and Moreira Gomes 2012).

The best-known function of PDFs is their antifungal activity (Lacerda et al. 2014). Positively charged PDFs can bind to negatively charged fungal phospholipids on cell surfaces (Järvå et al. 2017). According to the lipid/defensin complex model (Brogden 2005), PDFs integrate into pathogen membranes, form pore complexes and destroy membrane integrity. It is also assumed that some PDFs can intervene in transcriptional regulation. The PDF *Ps*D1 from pea is thought to enter the fungal cell nucleus and interact with proteins involved in cell cycle control (Lobo et al. 2007). PDF *Vv*AMP1 from *Vitis vinifera* strongly impairs fungal hyphae elongation (De Beer and Vivier 2011). Biological activities of PDF against herbivores include blocking of Ca^{2+} channels in vertebrates (Spelbrink et al. 2004) and inhibiting α-amylase activity in insects (Parisi et al. 2019).

In addition to the biotic defence mechanisms, PDFs are known to be involved in plant response to abiotic stresses such as drought (e.g., Dhn8 from *Glycine max*), low temperatures (Tad1 from *Triticum aestivum*), high soil salinity (various defensins from *Tabacum*; Lay and Anderson 2005), SO_2 exposure PDF1.2 of *A. thaliana*; (Hamisch et al. 2012) and heavy metals (*Ah*PDF1 of *Arabidopsis helleri*; Mirouze et al. 2006).

The broad spectrum as effectors against different stressors and their specific regulation make PDFs promising candidates for developing a system for the early stress detection in trees (Nosenko et al. 2021). Such a method would be essential for effective forest management to prevent large-area forest dieback. Facing increasing biotin and abiotic stress from global climate change and pathogen attack, early molecular/biochemical recognition of stress before the appearance of visible symptoms will constitute a significant advantage in forestry (Nosenko et al. 2021).

Due to inadequate correlation between transcriptome and proteome data in stress response (Guerrero-Sánchez et al. 2021), an AMP detection at the protein level is essential. The detection and quantification of PDFs has so far been attempted using polyclonal antibodies, e.g., in potato, tobacco or rice (Gao et al. 2000; Jha and Chattoo 2009; Van Der Weerden et al. 2008). However, highly specific monoclonal antibodies against two different epitopes for the enzyme-linked immunosorbent assay (ELISA) are required for the correct detection of the structurally very similar AMPs in crude plant extracts (Uotila et al. 1981).

Our aim was to establish a generalised biotechnological concept for the construction of test systems enabling the early detection of environmental stress in plants based on the detection and quantification of AMPs by ELISA (Figure 1). In this study, we use PDFs as stress marker molecules. As a model organism for defensins in trees, we chose *Fagus sylvatica* of the order Fagales (Yusypovych 2016), an economically and ecologically important European deciduous tree species that is increasingly under stress due to climate change.

We produced monoclonal antibodies by antibody phage display (Breitling et al. 1991) derived from the naïve human antibody library HAL9/10 (Kügler et al. 2015) by panning on recombinant PDFs in solution (Heine et al. 2023). Using a characterized sandwich antibody pair, we detected upregulation of *Fs*PDF2, the most abundant defensin in beech in response to biotic stress by gall midges. Our approach could be used by practitioners as a blueprint for the generation and application of antibodies against AMP for stress diagnosis.

2 | Methods

2.1 | Computational Prediction of Defensin- and Defensin-Like Gene Models in the *Fagus sylvatica* Genome

F. sylvatica reference genome sequence assembly v.1.3 (Mishra et al. 2018) was screened with FastBlockSearch, a search algorithm integrated into Augustus (Stanke et al. 2008) to identify potential genomic regions encoding defensins and defensin-like proteins. Amino acid profiles were constructed based on multiple sequence alignments of plant defensins from Silverstein et al. (2005) and Liu et al. (2017) and updated with sequences

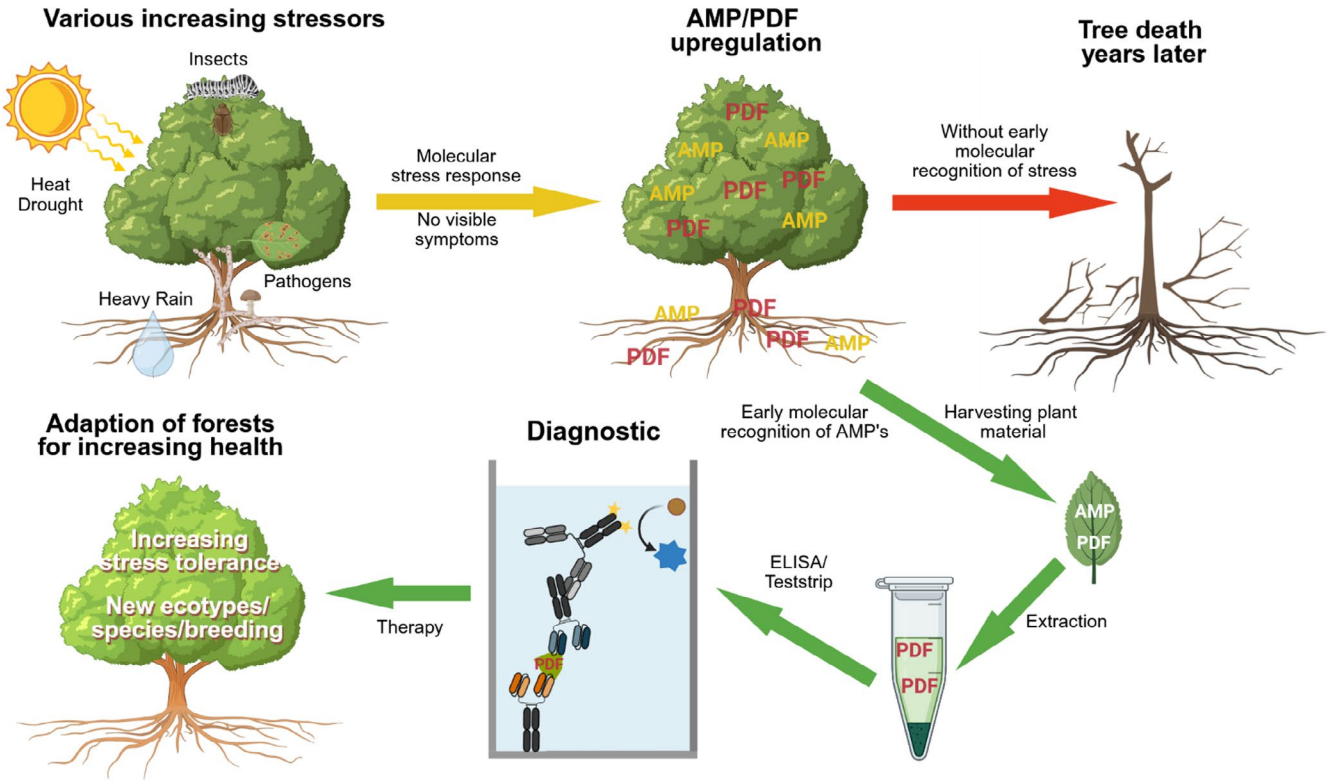

FIGURE 1 | Antimicrobial peptides (AMPs) such as plant defensins (PDFs) as diagnostic tools for early detection of stress in trees. Various stress factors threaten the health and fitness of trees with increasing intensity. Trees upregulate AMPs as an early molecular/biochemical immune response to stress before visible damage occurs. The diagnostics of AMPs by ELISA in plant tissue extracts, therefore, helps to initiate countermeasures in forestry at an early stage of tree damage and to identify plant species or genotypes with improved stress tolerance.

of putative defensin genes from the Fagaceae species *Quercus suber* and *Castanea sativa* (Data S1). The sequence alignments were converted into protein profiles using the msa2prfl.pl script integrated into Augustus. Annotation of putative defensin genes in the identified genomic regions was performed using Augustus-PPX (Protein Profile eXtension of Augustus) based on protein profiles that found high-score matches in the *F. sylvatica* genome. The Augustus parameters for *F. sylvatica* were determined using the Augustus Bioinformatics Web Server (http://bioinf.uni-greifswald.de/webaugustus/). *F. sylvatica* reference genome annotation v.1.3 (Mishra et al. 2018) was provided as a training set for parameter optimisation. An analysis of the overlap between the gene models predicted for each protein profile was performed and a unique set of defensin gene models was generated using the R package GenomicRanges (Lawrence et al. 2013). Similarly, GenomicRanges were used to find overlaps between the resulting unique set of defensin gene models predicted using Augustus-PPX and *F. sylvatica* reference genome annotation v.1.3. To identify N-terminal secretory protein splice sites, amino acid sequences of predicted defensins were analysed with SignalP (Nielsen 2017). Functional annotation of the predicted gene models was conducted using sequence similarity searches (BLAST (Camacho et al. 2009)) against the standalone NCBI nr database (National Center for Biotechnology Information Bethesda (MD): National Library of Medicine (US)) and *F. sylvatica* annotation v.1.3 gene models. Models of defensin genes expressed in leaf samples were verified based on alignments of RNA-Seq reads (see below) to the reference genome using Integrated Genomics Viewer (IGV; Robinson et al. 2011). The secondary structure of proteins encoded by these genes was verified using JPred (Drozdetskiy et al. 2015).

2.2 | RNA-Seq Data Generation and Analyses

Leaf samples were collected in May 2017 (forest near Rust, Germany; 48°15′55.2″ N 7°41′55.6″ E) from the crowns of four mature *F. sylvatica* trees, which showed varying degrees of infestation with *Phytophthora* spp. (Table S1). To ensure the diversity of biotic stress agents, only leaves damaged by herbivores were sampled. Total RNA was extracted from the leaf samples using the Spin Plant RNA Mini Kit (Stratec Molecular, Berlin, Germany) and purified from DNA using the TURBO DNA-free Kit (Ambion, Darmstadt, Germany). RNA concentration and integrity were assessed using Bioanalyzer 2100 (Agilent Technologies, Waldbroon, Germany). The preparation of random primed cDNA libraries was performed by KFB Sequencing Service of the University of Regensburg (Regensburg, Germany) according to the Illumina TruSeq Stranded mRNA Sample Preparation Guide (Illumina Inc., San Diego, CA, USA). Sequencing on the Illumina NextSeq 500 System in the paired-end mode with a read length of 2×100 bases was conducted by KFB Sequencing Service. The quality of all RNA-Seq libraries was assessed using FastQC v0.11.2 (Andrews 2010). Adapters, reads with average quality below 30 and low quality (<30) bases at the read termini were trimmed using Trimmomatic v0.36 (Bolger et al. 2014). Processed read pairs were aligned to the *F. sylvatica* reference genome sequence assembly using the

STAR v.2.5.2a (Dobin et al. 2013) aligner program. Read pairs aligned to exonic regions were summarised per gene using featureCounts (Liao et al. 2014) and *F. sylvatica* gene annotation v.1.3 merged with the Augustus-PPX annotation of putative defensin genes.

2.3 | Plant Material

Two sites in Brandenburg near Eberswalde (Germany) were selected to sample drought-stressed beech trees. The first beech forest near the village of Beerenbusch (53°08′20.0″ N 12°56′06.4″ E) had medium-coarse sandy-brown soil of medium nutritional value. The second beech locus near the village Britz (52°52′40.1″ N 13°50′06.5″ E) grows on Finowtal sandy brown soil of medium nutritional value. The harvest occurred in September 2019 after a long summer drought period. The control trees were located directly beside the lake nearby (Britz: 52°52′26.9″ N 13°50′23.9″ E, Beerenbusch 53°08′20.0″ N 12°56′06.4″ E), and therefore, had direct access to water without being exposed to flooding stress.

To define the actual drought stress on-site, water potential measurements were carried out using a Scholander vessel (Scholander et al. 1965). For this purpose, sampling was conducted between 10 and 12 am local time to exclude any daytime-dependent effects. Thin twigs with leaves were collected from the trees, and 20 leaves were immediately stored in liquid nitrogen.

Gall midge tumors were collected from leaves in a forest near Braunschweig (Germany; 52°19′18.8″ N 10°20′31.6″ E). After separation from the surrounding leaf tissue, tumors were frozen directly in liquid nitrogen. The remaining leaf material was also deep-frozen directly on site.

Leaf tissue or gall midge tumours were ground in liquid nitrogen before adding 500 µL PBS extraction buffer (10 mM Na_2HPO_4, 1.8 mM KH_2PO_4, 137 mM NaCl, 2.7 mM KCl, 2% polyvinylpyrrolidone, 1% NP-40, 2% PMSF and 1% proteinase inhibitor cocktail for plant extracts (Merck KGaG, Darmstadt, Germany), pH 7.4) to 100 mg of plant material. After briefly inverting, sonication of samples in a pre-cooled ultrasonic bath was performed twice for 15 s. Beech embryos were separated from the endosperm of beech nuts. 500 µL PBS extraction buffer was added to each embryo before cell disruption using a grinding mill (Precellys 24; PeqLab, Erlangen, Germany) with porcelain beads twice for 30 s with 5 s interruption. All samples were freeze cracked, with an incubation for 1 min in liquid nitrogen and 1 min in a 37°C warm water bath. This cycle was repeated 3 times. After that the samples were inverted and centrifuged twice at 16 600×*g* at 4°C for 10 min. The protein concentration was measured with RotiQuant (Carl Roth GmbH & CoKG, Karlsruhe, Germany) according to the manufacturer's protocol.

2.4 | Quantitative Real-Time PCR

For total RNA extraction, InviTrap Spin Plant RNA Mini Kit (Invitek Molecular GmbH, Berlin, Germany) was used according to the manufacturer's protocol with slight modifications. Briefly, 30 mg freeze-dried powder was added to 500 µL of LRP (lysis) buffer augmented with 1% (v/v) β-mercaptoethanol, 1% (w/v) PVPP, vigorously vortexed and incubated at room temperature for 15 min. After treatment with Turbo DNase Free Kit (Life Technologies GmbH, Darmstadt, Germany), extracts were placed directly onto an RNA Spin Filter, treated according to the manufacturer's protocol. RNA quantity and quality were verified with Nanodrop 1000 (Life Technologies GmbH, Darmstadt, Germany) and agarose gel electrophoresis (2 bands of 18 s and 28 s rRNA). The first strand cDNA was synthesised using 200 ng of RNA and the iScript cDNA synthesis Kit (BioRad, Hercules, California).

Primers were designed with Primer3 (Kõressaar et al. 2018) using adjusted default settings. The 18S rRNA Reference Gene primer was designed using the *F. sylvatica* gene partial sequence (GenBank: AJ888473.1; Mishra et al. 2018) by the same designing platform.

The RT-qPCR assays were performed using LightCycler 480 SYBR Green I Master Mix on LightCycler 480 (Roche Diagnostics GmbH, Mannheim, Germany). All qPCR was performed using SYBR Green and was conducted at 95°C for 5 min, and then 40 cycles of 95°C for 10 s, 56°C for 10 s and 72°C for 12 s. Relative gene expression pattern was analysed as described by Livak and Schmittgen (2001) by the $2^{-\Delta\Delta C_t}$ method after normalising with the reference gene (18 s rRNA) and plotted on a log scale.

2.5 | *Fs*PDF2 Vector Cloning

The recombinant *Fs*PDF2 was designed with a TEV protease cleavage site and a twinStrepTag linked by a glycine-serine linker to the protein (Figure S1). The codon-optimised sequence was cloned with *Hin*dIII and *Not*I in the OpiE2 vector (Table S2), including a signal peptide for secretion (Bleckmann et al. 2015; Korn et al. 2020).

2.6 | Recombinant Production and Purification of *Fs*PDF2 in Insect Cells

High Five (BTI-Tn-5B1-4) insect cells (Thermo Fisher Scientific, Waltham, USA) were used to produce *Fs*PDF2 baculovirus-free by transient plasmid transfection as described before (Korn et al. 2020). The supernatant was harvested 96 h after transfection by two-step centrifugation (4 min at 180×*g*, followed by 20 min at 3 220×*g*). *Fs*PDF2 was purified with His Mag Sepharose Excel beads (Cytiva, Marlborough, USA) or automatically with the Äkta system (Cytiva, Marlborough, USA) according to the manufacturer's protocol. The purity was monitored by the Äkta system and SDS-PAGE.

2.7 | Antibody Selection With Phage Display

Phage display panning was performed in solution using the naïve HAL9 and HAL10 human antibody libraries (Kügler et al. 2015) in three rounds, followed by one round with an immobilised antigen. For the first panning round, the library was packaged using Hyperphage (Rondot et al. 2001; Soltes et al. 2007). The panning in solution was performed according

to Heine et al. (2023) with modifications. Briefly, 5×10^{10} cfu (cell forming units) of each library was diluted in 150 μL 2% (w/v) BSA-PBST and separately preincubated in an MTP well blocked with a panning block (1% BSA and 1% milk powder in PBST). StreptactinXT (IBA-Lifesciences GmbH, Göttingen, Germany) beads were prepared. After that, the libraries were preincubated on 10 μL bead slurry in a total volume of 600 μL 2% BSA in PBST in a low-binding Eppendorf tube for 1 h in a tube rotator at room temperature (RT). Magnetic beads were separated for the panning procedure, and 1 μg antigen was added to the supernatant. The panning reaction was incubated for 90 min at RT. After that, 10 μL washed StreptactinXT bead suspension was added for magnetic pulldown. The reaction was incubated for 30 min at RT, the supernatant was discarded, and the beads were washed 10 times with 1 mL PBST. Beads were washed 20 times and 30 times in the second and third panning rounds. After washing, the remaining phages were eluted in 200 μL trypsin (10 μg/mL in PBS) for 30 min at 37°C and separated from the beads. The fourth panning round was performed with 1 μg *Fs*PDF2 immobilised on MTP to add a non-related antigen with a twin-StrepTag for soluble competition for depletion of twinStrepTag binding scFv clones.

For monovalent phage amplification, 100 μL eluate was used to infect 500 μL *E. coli* XL1 Blue MRF' (Invitrogen, Waltham, Massachusetts) for 30 min at 37°C. Bacteria were plated on 2xYT-GA agar plates and incubated overnight at 37°C. The next day, colonies were scrabbed with 5 mL 2xYT media from the plate and used for inoculation at $OD_{600} = 0.1$. Bacteria were incubated at 37°C until they reached an $OD_{600} \approx 0.5$ and infected with M13K07 helper phage for 30 min at 37°C, followed by 30 min at 37°C with shaking to express antibiotic resistance. After centrifugation, media was changed to 2xYT-KA, and bacteria were incubated at 37°C and 350 rpm overnight for phage production. The phages were precipitated with PEG/NaCl, titrated and used for the next panning round.

After the fourth panning round, to identify binders in screening-ELISA, monoclonal single chain-Fv (scFv) fragments were produced from picked individual clones in a 96-well microtiter plate (MTP). These fragments were screened in respect of binding on the desired antigen *Fs*PDF2 and an unrelated negative control protein, respectively. Clones binding specifically were sequenced and produced in scFv-Fc antibody format (Heine et al. 2023).

2.8 | Recombinant Antibody Production

Selected scFv clones were cloned into pCSE2.6-hIgG1-Fc and pCSE2.6-mIgG2a-Fc vectors using *Nco*I and *Not*I to produce scFv-Fc fusion proteins as described (Wenzel et al. 2020).

The scFv-Fc antibodies were produced in Human Embryo Kidney (HEK) Expi293F cells (Thermo Scientific, Waltham, Massachusetts, USA) in a 5 mL scale. The cells were cultivated at 37°C, 110 rpm, and 5% CO_2 in Gibco Freestyle F17 media (Thermo Scientific). The medium was supplemented with 8 mM L-glutamine and 0.1% Pluronic F68 (PAN Biotech, Aidebach, Germany). Cells were transfected with polyethylenimine (PEI) at a density of $1.8–2.2 \times 10^6$ cells/mL and a viability above 90%. For transfection, 1 μg of DNA was mixed with 5 μg of 40 kDa PEI (Polyscience, Warrington, USA) in 5% transfection volume in the medium. The mix was incubated for ca. 25 min at RT and added to the cells. After 48 h, the cells were fed with 5 mL HyClone SFM4Transfx-293 medium (GE Healthcare, Chicago, Illinois) supplemented with 8 mM L-glutamine and 1 mL Hyclone Boost 6 supplement (GE Healthcare, Chicago, Illinois). One week after transfection, the cells were harvested by centrifugation for 15 min at 1500×*g* (Bertoglio et al. 2021).

The scFv-Fc fusion proteins were purified by Protein-A with MabSelect SuRe (GE Healthcare, Chicago, Illinois) according to the manufacturer's manual. Production and purity were verified by SDS-gel electrophoresis.

2.9 | Titration ELISA

*Fs*PDF2 concentration in crude plant extract was determined using a sandwich ELISA assay to enrich the analyte. A capture antibody binds *Fs*PDF2 specifically, while the rest of the unspecific proteins in the extract are washed away. Subsequently, the primary antibody is used for defensin detection.

Titration ELISA was performed in 96-well MTP plates (Greiner Bio-One GmbH, Frickenhausen, Germany). Antigen or antibodies were immobilized overnight at 4°C (400 ng in 100 μL PBS per well). After washing (Titertek ELx405); (program 3xC), Biotek Instruments, Winooski, Vermont, USA), the remaining binding sites on the polystyrene surface in the MTP wells were blocked with 330 μL/well blocking solution (2% polyvinylpyrrolidone (PVP) (w/v) in PBS) for 1 h at RT. The plates were washed before the titrant (diluted in working solution (1% BSA (w/v), 1% PVP (w/v) in PBST (PBS with 0.05% Tween-20)) was directly titrated in the MTP in 100 μL/well working solution from the highest concentration to the lowest, according to the experimental setup. Plates were incubated for 1 h at RT. After washing, the primary antibody for *Fs*PDF2 detection was added in 100 μL M-PBST/well and incubated for 1 h at RT, followed by washing and incubation with secondary antibody for detection, either Fc-part specific, HRP coupled goat anti-human-IgG (A0170; Sigma-Aldrich, St. Louis, USA) or goat anti-mouse-IgG (A0168; Sigma-Aldrich, St. Louis, USA), depending on the species of the primary antibody. After final washing, the HRP was detected by 3,3′,5,5′-Tetramethylbenzidine (TMB). The reaction was stopped after 15–30 min with 1 N sulfuric acid. The absorption (OD) difference between $OD_{450\ nm}$ and $OD_{620\ nm}$ was measured with an Epoch reader (Biotek Instruments, Winooski, Vermont, USA). The effective concentration at 50% signal (EC_{50}) was computed with OriginPro (OriginLab, Northampton, Massachusetts), using the five-parameter logistic fit.

2.10 | In Silico Analysis Using ColabFold

To investigate the structure prediction of the antibody–antigen complex, we utilised ColabFold v.1.5.3 (Mirdita et al. 2022) and the AlphaFold 3 servers provided by Google (Abramson et al. 2024). The sequence queries contained the amino acid sequences of the scFvs generated in this study via phage display and the anticipated sequence of the *Fs*PDF2 protein without its

predicted signal peptide. Multiple Sequence Alignment (MSA) was executed using MMseqs2 (UniRef + Environmental) with an unpaired plus paired strategy. Each model underwent at least five cycles, and the top-ranking models, surpassing a 75% confidence threshold, were employed for subsequent visualisation and superposition of the structure using UCSF ChimeraX (Pettersen et al. 2021).

The initial AlphaFold prediction runs utilised the amino acid sequences of both scFvs (PHE148-H1, PHE183-B12) and *Fs*PDF2 (Figure S2). However, we recognised a potential flaw in this approach: AlphaFold, while highly efficient, does not inherently consider a potential steric hindrance effect between antibodies occupying nearby epitopes. Consequently, we modelled each scFv separately with *Fs*PDF2 and superimposed the predicted *Fs*PDF2 structures.

2.11 | Transient Transformation of *Nicotiana benthamiana*

The coding sequences of *F. sylvatica* defensin *Fs*PDF2 were amplified by PCR from *F. sylvatica* cDNA using *attB* site-flanked primers to allow recombination of the respective PCR product into the pDONR/Zeo vector by BP reaction using the GATEWAY cloning system (Invitrogen, USA). For localization studies, the resulting entry vector was used for LR recombination into pK7WG2 (Karimi et al. 2002), generating the expression vector pExp-*fspdf2*. The negative control generation was described by (Weber et al. 2021). The genomic region of the promoter was amplified and subcloned into pDONR/Zeo via BP-reaction to generate entry vectors. Recombination of these entry vectors via LR reaction with the pKGWFS7 destination vector (Karimi et al. 2002) resulted in the expression vector pEndo- *mot2.1*::*gus* coding for a GFP-GUS fusion protein. *Agrobacterium*-mediated transient expression in leaves of *N. benthamiana* was performed as described by (Kaufholdt et al. 2013). *Agrobacterium tumefaciens* harboring the expression vectors were co-infiltrated into the intercellular space of plant leaves. For optimal comparison, the defensin and negative control approaches were infiltrated in one leaf of a leaf pair each.

2.12 | Co-Immunoprecipitation (CoIP) and Protein Identification by Mass Spectrometry (MS)

To evaluate the specificity of the antibodies PHE148-H1 and PHE183-B12, co-immunoprecipitation with protein identification by MS was performed. Protein extracts from gall midge tumours and recombinantly produced *Fs*PDF2 were used for these experiments. Protein extraction from gall midge tumours was performed as described above. 20 µg antibodies were bound to Pierce Protein A/G Magnetic Beads (Thermo Scientific; Ref.88802) according to the manufacturer's instructions with some modifications. In brief, beads were incubated with the antibodies for 1 h at room temperature.

Besides PHE148-H1 and PHE183-B12, beads were coated with the antibody SH1956-D6 (specific for an *Arabidopsis thaliana* defensin). SH1956-D6-coated beads and beads without antibody served as controls for non-specific protein binding. A total of 500 µg proteins from the gall midge extracts or 37.5 µg of recombinant *Fs*PDF2 were used for co-immunoprecipitation. Each sample was made up to a volume of 500 µL with extraction buffer. After overnight incubation of the beads with the protein extracts at 4°C and gently mixing at 25 rpm on a spinning wheel, beads were collected and washed with Tris-buffered saline (TBS pH 7.5, Product No. 28360) containing 0.05% Tween-20.

Proteins were eluted from the beads using 100 µL elution buffer containing 0.8% (w/v) Tris–HCl (pH 6.8), 5% (v/v) β-mercaptoethanol, 15% (v/v) glycerol, 2.4% (w/v) SDS, 0.4% (w/v) bromophenol blue. Protein digestion with trypsin was performed in protein low binding tubes (Eppendorf, Hamburg, Germany) using the Single-Pot Solid Phase Sample Preparation technique (SP3) previously described (Hughes et al. 2014) with modifications according to Mateus et al. (2018). Peptide purification was carried out as described by Fuchs et al. 2021 using Oasis HLB-SPE-cartridges (1 cc, 10 mg, Waters, Milford, MA, USA). Peptides were eluted sequentially with 13% (v/v) acetonitrile, 25% (v/v) and 75% (v/v) acetonitrile in 0.5% (v/v) formic acid. The three fractions were combined, and an aliquot (one tenth of a sample) was additionally desalted using ZipTips (C18, Merck Millipore, Billerica, MA, USA) as described previously (Fuchs et al. 2021). After sample preparation for liquid chromatography/tandem mass spectrometry (LC–MS/MS) analysis according to (Fuchs et al. 2021), LC–MS/MS runs were performed on a nanoAQUITY Ultra Performance Liquid Chromatography System (Waters Corporation, Milford, MA, USA) that was coupled to an LTQ Orbitrap Velos Pro mass spectrometer (Thermo Fisher Scientific Inc) using a 125 min gradient at a flow rate of 0.35 µL/min starting with 3.7% buffer B (80% (v/v) acetonitrile and 0.1% (v/v) formic acid) and 96.3% buffer A (0.1% (v/v) formic acid in UltraLC–MS water): 0–30 min 3.7% buffer B; 30–60 min 3.7%–31.3% buffer B; 60–100 min 31.3%–62.5% buffer B; 100–108 min 62.5%–90% buffer B; 108–113 min 90% buffer B; 113–118 min 99%–3.7% buffer B, 118–125 min 3.7% buffer B.

Primary MS scans were performed in the Orbitrap scanning an m/z range of 350–1800 with a resolution of 60 000 and a lock mass of 445.12003. Primary ions were fragmented in a data-dependent collision-induced dissociation (CID) mode for the 10 most abundant precursor ions with an exclusion time of 24 s and analysed using the LTQ ion trap. Ionisation parameters were set according to Fuchs et al. (2021).

Analysis of the raw MS data was conducted using MaxQuant (version 2.4.3.0; Max Planck Institute of Biochemistry, Martinsried, Germany) with the parameters described previously (Fuchs et al. 2021) and a FASTA file containing all known *Fagus sylvatica* proteins, downloaded from Uniprot on 2024-05-08, combined with protein sequences for the human and the mouse antibody specific for *Fs*PDF2 (PHE148-H1, PHE183-B12) as well as for the IgG binding proteins A and G (Uniprot on 2025-01-29). All contaminants were removed from the list of identified proteins. Only proteins with at least two MS2 counts and a ratio between protein intensity and the number of unique peptides of at least 100 000 were considered to be reliably identified. In the case of proteins with more than 100 amino acids, a minimum of two unique peptides had to be detected. The filter criteria described by Fuchs et al. (2021) were applied to reliably identify proteins with up to 100 amino acids, except that the detection

of the proteins was only required in one sample. iBAQ values provided by MaxQuant were used for quantitative comparisons.

The mass spectrometry proteomics data have been deposited to the ProteomeXchange Consortium via the PRIDE partner repository (Perez-Riverol et al. 2025) with data set identifier PXD060631 (https://www.ebi.ac.uk/pride/archive, username: reviewer_pxd060631@ebi.ac.uk, password: bspWmsVfw9Vw). Alternatively, reviewers can log in to the PRIDE website using the following details: Project accession: PXD060631, Token: SNgbaUCar5PD.

3 | Results

3.1 | Beech Defensin- and Defensin-Like Gene Prediction and Expression Analyses

Eighty loci putatively encoding defensin-like proteins were identified in the *Fagus sylvatica* genome using AUGUSTUS-PPX and amino acid alignments of plant defensins (Liu et al. 2017; Silverstein et al. 2005) (Data S2, Table S1). Fifty-seven of them contained a signal peptide (SP) characteristic of the defensin-like genes. Only five of these models overlapped with gene models from the *F. sylvatica* genome annotation v. 1.3.

To identify defensin-like genes involved in the response to biotic stress, we generated four RNA-Seq libraries using RNA extracted from leaves visibly damaged by herbivores. For this purpose, leaves were collected from four mature *F. sylvatica* trees characterised by different degrees of *Phytophthora* infection. Only two of the predicted defensin-like genes, CRP0000-1 and CRP01104-12, had relatively high expression levels in all samples (see Table S1). CRP01104-12 likely represents an expressed pseudogene as it lacks SP. CRP0000-1 overlaps with the defensin Ec-AMP-D2-like gene model FSB0104284 from *F. sylvatica* genome annotation v.1.3. It has primary and secondary amino acid sequence structures that are typical for plant defensins. We call this gene *Fs*PDF2 (*F. sylvatica* Plant Defensin 2). *Fs*PDF2 was selected for further analyses as a potential stress biomarker candidate.

3.2 | Recombinant *Fs*PDF2 Production and Antibody Generation

*Fs*PDF2 was produced in a baculovirus-free High Five insect cell system. After purification by His8 tag via IMAC, a maximum yield of 7.8 mg/L could be obtained. The recombinant protein was stable for 4 weeks under different storage conditions (Figure S3). Due to the small size of *Fs*PDF2, monoclonal recombinant antibody generation was achieved by phage display using panning in solution with a magnetic bead pulldown (Figure 2a) to mitigate potential steric hindrances or denaturation of conventional plate-based panning. During the panning process, specific binding scFv fragments against *Fs*PDF2 are enriched from each round to another, whereas unspecific binders are depleted due to preclearance of the libraries, and non-binders are eliminated with harsh washing. With the additional fourth panning round on MTP, a counterselection with an unrelated antigen against the twinStrepTag was performed to deplete scFv fragments binding the tag. Seven unique scFv fragments were identified: two clones with lambda light chains and five with kappa light chains.

The binding performance of scFv antibodies was further characterised by titration ELISA and ranked based on EC_{50} values (Figure 2b). All antibodies showed a similar binding strength to the antigen with an EC_{50} value in a picomolar range, except PHE183-F1, whose EC_{50} was in the low nanomolar range (Table 1). The similarity of the complementarity determining regions (CDRs) of the antibodies indicates that all kappa antibodies bind to the same epitope, whereas lambda antibodies bind to a different one. Although the generated antibodies are therefore very well suited for use in ELISA, it was not possible to demonstrate their applicability in reducing and native Western blots (compare Tomisawa et al. (2013)).

Different antibody combinations in the scFv format were tested and ranked based on their EC50 value to develop a *Fs*PDF2 sandwich ELISA, necessary to measure defensin concentration in crude plant extracts. The best-performing kappa antibodies, PHE148-H1, PHE182-D5 and PHE182-E2, were used to capture the antigen, while the best-performing lambda antibody PHE183-B12 was used as the detection antibody. All three combinations had EC_{50} values in a similar low nanomolar range (Figure 2c). For the subsequent ELISA studies, we used the combination of PHE148-H1 and PHE183-B12, which resulted in a combined EC_{50} of 8 nmol. A co-immunoprecipitation with recombinant *Fs*PDF, followed by a LC–MS/MS analysis demonstrated the specific binding capability of both antibodies (Table S3).

3.3 | PHE148-H1 and PHE183-B12 Bind *Fs*PDF2 at Distinct Epitopes

We utilised AlphaFold 3 to predict the antibody–antigen–antibody complex (Abramson et al. 2024). Each scFv was modelled individually in complex with *Fs*PDF2. The *Fs*PDF2 structures were superimposed to generate a comprehensive complex model (Figure 3a). For structure reliability, the predicted Local Distance Difference Test (pLDDT) confidence scores and the interface predicted template modelling (ipTM) score were used (Xu and Zhang 2010; Zhang and Skolnick 2004). The pLDDT scores for the CDR regions exceeded 80, while the *Fs*PDF2 fragment scored above 70. The ipTM score was 0.74 for PHE148-H1 in complex with *Fs*PDF2 and 0.71 for PHE 183-B12 in complex with *Fs*PDF2.

As predicted by AlphaFold, the HAL10 derived scFv (PHE148-H1, PHE182-D10, PHE182-D5, PHE182-E11, and PHE182-E2) with kappa light chain binds to the same epitope of *Fs*PDF2 (Figure S4). The epitopes of *Fs*PDF2 were determined by analysing the CDR regions as interface templates. PHE148-H1 in complex with *Fs*PDF2 revealed an interface mostly directed by VH CDR-2 and CDR-3 targeting the gamma core motif of *Fs*PDF2 (epitope 1; TXV/RGFRRR) (Figure 3b). For PHE183-B12, the heavy and the light chains were predicted to bind fully to the single alpha helix characteristic for defensins, resulting in *Fs*PDF epitope 2 (RXQ/RXSNXXXAVXQTE) (Figure 3c). These results confirm that PHE148-H1 and PHE183-B12 bind *Fs*PDF2

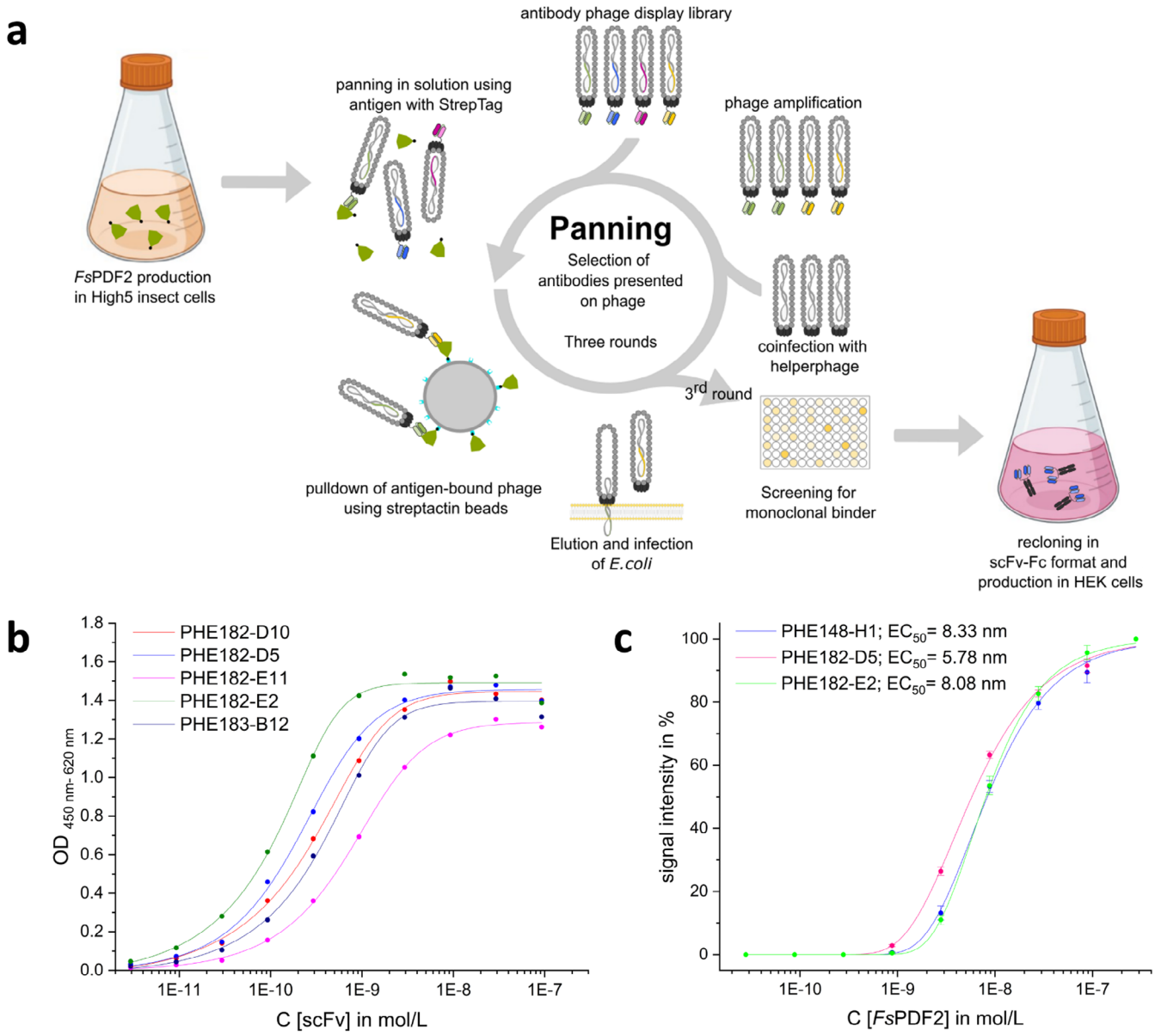

FIGURE 2 | Antibody selection with phage display and characterisation of binders. (a) Panning in solution to select specific antibodies against *Fs*PDF2. The naïve human antibody libraries HAL9 and HAL10 were incubated with the tagged *Fs*PDF2 in solution. After a tag-based pulldown of the antigen and a harsh washing, bound phages were eluted, and *E. coli* cells were infected. For the next panning round, new phages were packaged with a helper phage. After three rounds of panning in solution and one panning round with immobilised antigen on a microtiter plate, scFv were screened for binding. Binders were cloned into a scFv-Fc format and produced in HEK Expi293F cells (modified from Wenzel et al. (2020)). (b) Generated scFv-Fc antibodies have different binding performances on immobilised *Fs*PDF2. The EC_{50} values range from 0.13 to 0.79 nmol/L. (c) *Fs*PDF2 Sandwich ELISA using PHE183-B12 as detection antibody while FsPDF2 was immobilised by the three best-performing kappa antibodies ($n = 3$).

at distinct epitopes, providing insights into their ability to be used within a sandwich ELISA.

3.4 | Detection of Recombinant *Fs*PDF2 in Plant Material

To confirm the detection in plants, *Fs*PDF2 without tags was transiently overexpressed in *Nicotiana benthamiana* by transformation with *Agrobacterium tumefaciens*. This material was used to test the sandwich ELISA (Figure 4a) with plant extract. The defensin could be detected in the ELISA at total protein concentrations higher than 10 µg/mL. A background signal was generated at protein concentrations above 100 µg/mL (Figure 4b). This background signal could be due to the weak cross-reaction of the antibodies with homologous *N. benthamiana* defensins in the plant extract. This assumption is promoted by an increased signal after Agrobacterium-induced immune reaction of the plants.

Within the linear range of the calibration curve of recombinant *Fs*PDF2 (Figure 4c), we determined the defensin concentration of beechnuts to be between 15 and 50 ng per embryo and between 5 and 18 µg per g embryo fresh weight (Figure 4d).

TABLE 1 | Monoclonal recombinant antibodies against *Fs*PDF2 generated by phage display against *Fs*PDF2. The highlighted antibodies are used in the following analysis.

Antibody clone	Library	EC_{50} in nmol
PHE148-H1	**HAL10 (kappa light chain)**	**0.17**
PHE182-D10	HAL10 (kappa light chain)	0.32
PHE182-D5	HAL10 (kappa light chain)	0.22
PHE182-E11	HAL10 (kappa light chain)	0.79
PHE182-E2	HAL10 (kappa light chain)	0.13
PHE183-B12	**HAL9 (lambda light chain)**	**0.4**
PHE183-F1	HAL9 (lambda light chain)	4.47

Leaf material contains many more secondary metabolites than embryos interfering with the ELISA assay (Figure S5). To adsorb especially tannins, the extraction was performed with polyvinylpyrrolidone (PVP) (Magalhães et al. 2010). We also observed higher ELISA signals by exchanging milk powder for PVP in the assay (Figure S6). After extraction with PVP, the calibration curve with recombinant *Fs*PDF2 showed similar absorbance values in PBS buffer, as well as in plant extract (Figure S7).

3.5 | Defensin Detection in the Natural Ecosystem by *Fs*PDF2 Sandwich-ELISA

Finally, We Used the Sandwich Antibody Set PHE148-H1 and PHE183-B12 to detect *Fs*PDF2 in samples from stressed ecosystems. Drought was chosen as an abiotic stressor. Leaf samples from mature trees were collected at two sites near Eberswalde (Germany) in 2019 after a dry summer period. The control trees were located at a nearby lake. Leaves of the control and the drought-exposed trees already differed in their visual appearance. Control trees had large green leaves, while drought-exposed trees had small yellowish leaves (Figure S8). Branch water potential in the

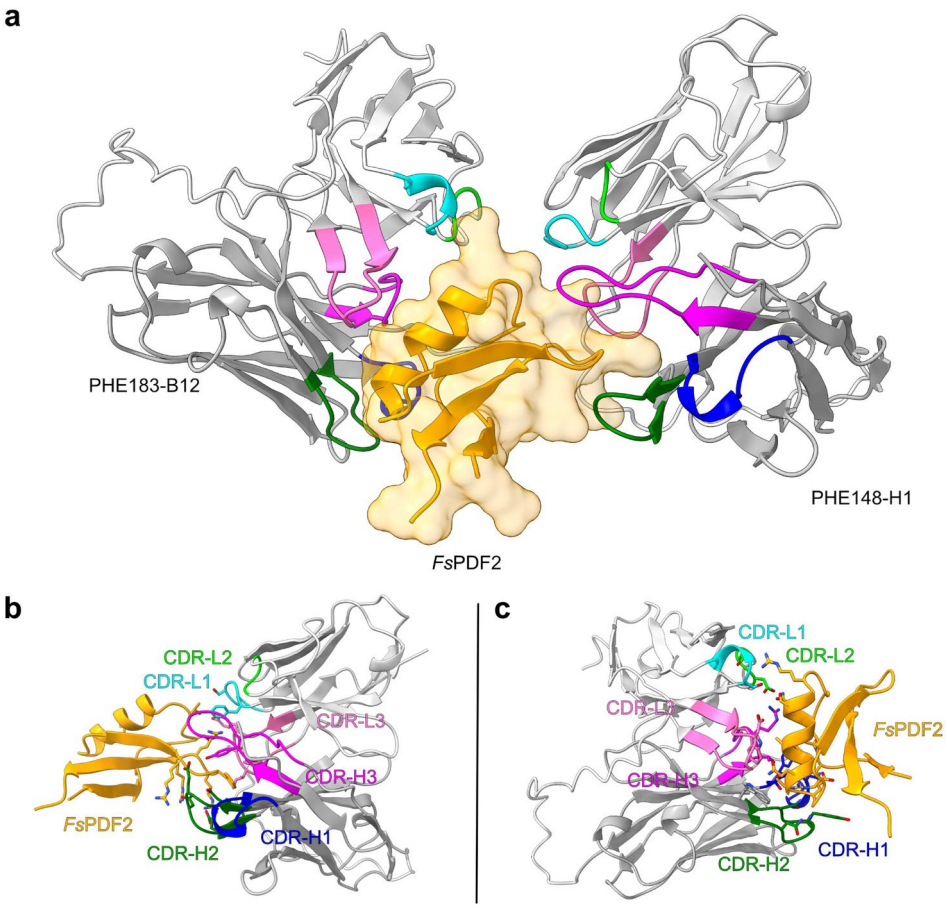

FIGURE 3 | Interaction of PHE148-H1 and PHE183-B12 with *Fs*PDF2. (a) Predicted protein structure of *Fs*PDF2 in complex with the scFv fragments PHE148-H1 and PHE183-B12. *Fs*PDF2 is coloured orange. The scFv heavy chains are coloured in dark grey, and the light chain in light grey. The CDR1 loops are coloured blue (H) and cyan (L), the CDR2 loops are coloured green (H) and lime (L), and the CDR3 loops are coloured magenta (H) and pink (L). (b) Interface of PHE148-H1 and FsPDF2. (c) Interface of PHE183-B12 and FsPDF2 displayed as seen for PHE148-H1. (b, c) To indicate the interface residues, we display the residues located no more than 3.0 Å away from their partner's surface as sticks.

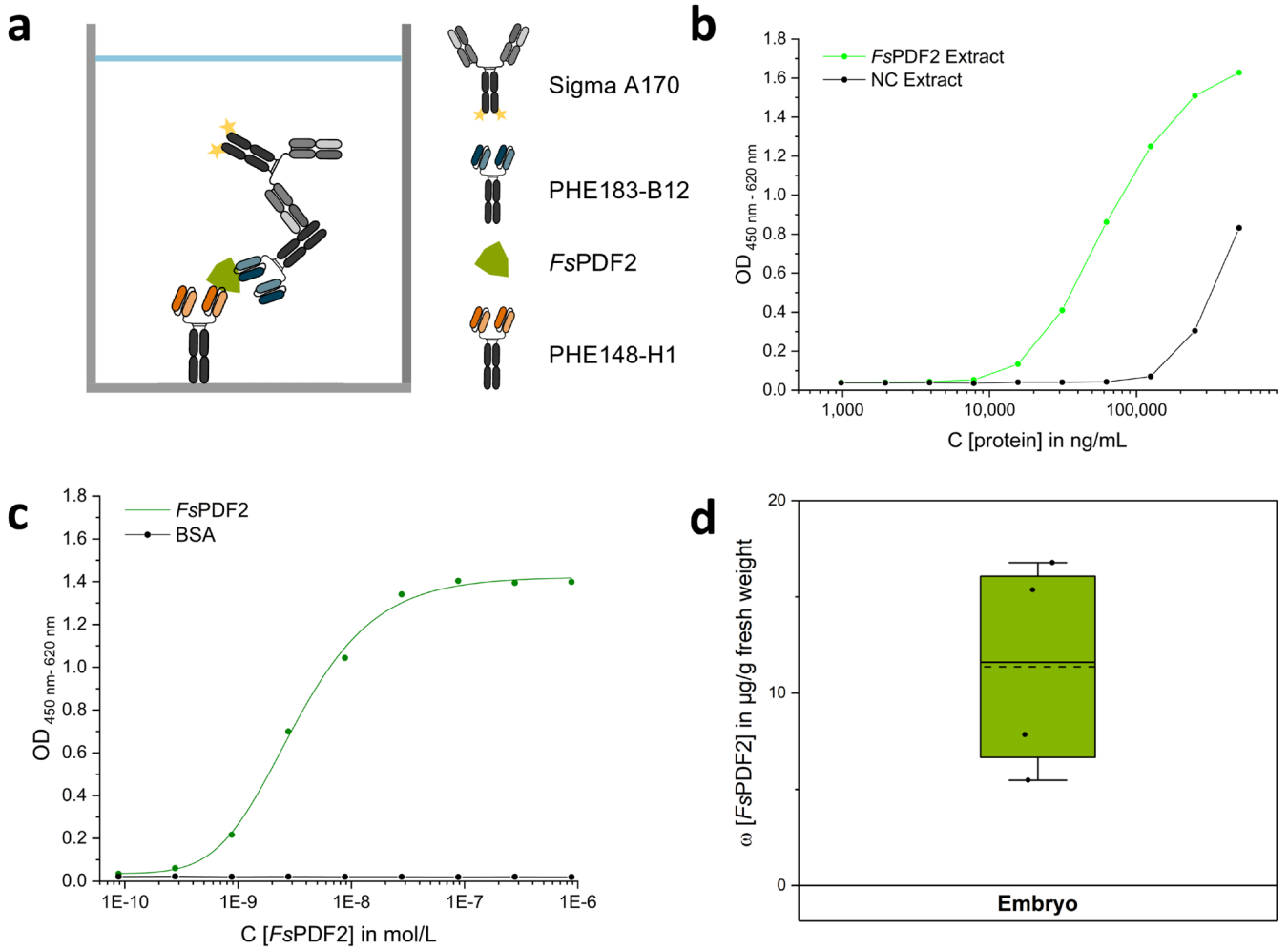

FIGURE 4 | Detection of *Fs*PDF2 in plant material. (a) Sandwich-ELISA setup for PDF and antimicrobial peptides (AMPs) detection in plant extracts. PHE148-H1 is immobilised to capture the *Fs*PDF2 out of the plant extract. PHE183-B12 binding the captured defensin is detected with a HRP labelled goat anti-human-IgG (Fc specific) antibody. (b) *Fs*PDF2 without any tags overexpressed in *N. benthamiana* extract is detectable above a total protein concentration of 10 µg/mL. Negative control (NC) extract (leaves transformed with ß-glucuronidase under the control of the mot 2.1 promoter) shows the background signal. (c) Titration curve with recombinant *Fs*PDF2 to determine the defensin concentration in *F. sylvatica* embryos. (d) *Fs*PDF2 concentration in beechnut embryo extracts ($n = 4$).

drought-exposed trees in Britz was significantly lower ($p = 0.001$) relative to the control (Figure 5a). Results of quantitative real-time PCR showed a 24-times enhanced transcription level of the gene encoding *Fs*PDF in leaves collected from drought-exposed trees in Beerenbusch (Figure 5b). Reduced protein content in the leaves of drought exposed trees is an additional indication of drought stress (Figure 5c). However, no significant *fs*PDF2 upregulation on protein level in the leaves of drought-stressed trees was detectable on both sites (Figures 5d and S9).

To investigate biotic stress, we used beech leaves infested with gall midges (*Cecidomyiidae* spp.). The galls and healthy beech leaf material around the galls were harvested. The defensin concentrations measured in galls were significantly higher ($p = 0.001$) than in the surrounding leaf areas (Figure 5f). Although the protein concentration of defensins in the galls was 3 times lower (Figure 5e), the amount of *Fs*PDF2 normalized to the protein content was 24 times higher in galls relative to the surrounding tissue. Co-immunoprecipitation experiments with subsequent LC-MS/MS analysis showed that the PHE148-H1 antibody can significantly enrich *Fs*PDF2 from the gall midge tumor extract, a strong indication that the antibody is highly specific for *Fs*PDF2. While confirming its specificity, the PHE183-B12 showed a significantly weaker signal in co-immunoprecipitation with the recombinant *Fs*PDF2 than the PHE148-H1 antibody, with *Fs*PDF2 from the gall midge tumor extract possibly remaining below the limit of detection in the co-immunoprecipitation (Table S3). However, a direct quantitative LC-MS detection of FsPDF2 was not feasible due to its low abundance and high background interference from secondary metabolites in crude plant extracts. Thus, ELISA remains the more suitable choice for practical and quantitative detection in complex plant matrices. Nevertheless, the results indicate a specific *Fs*PDF2 detention showing a strong stress response of the leaf tissue to the parasite.

4 | Discussion

Antimicrobial peptides (AMPs), such as plant defensins (PDFs), are involved in biotic and abiotic stress response regulation and

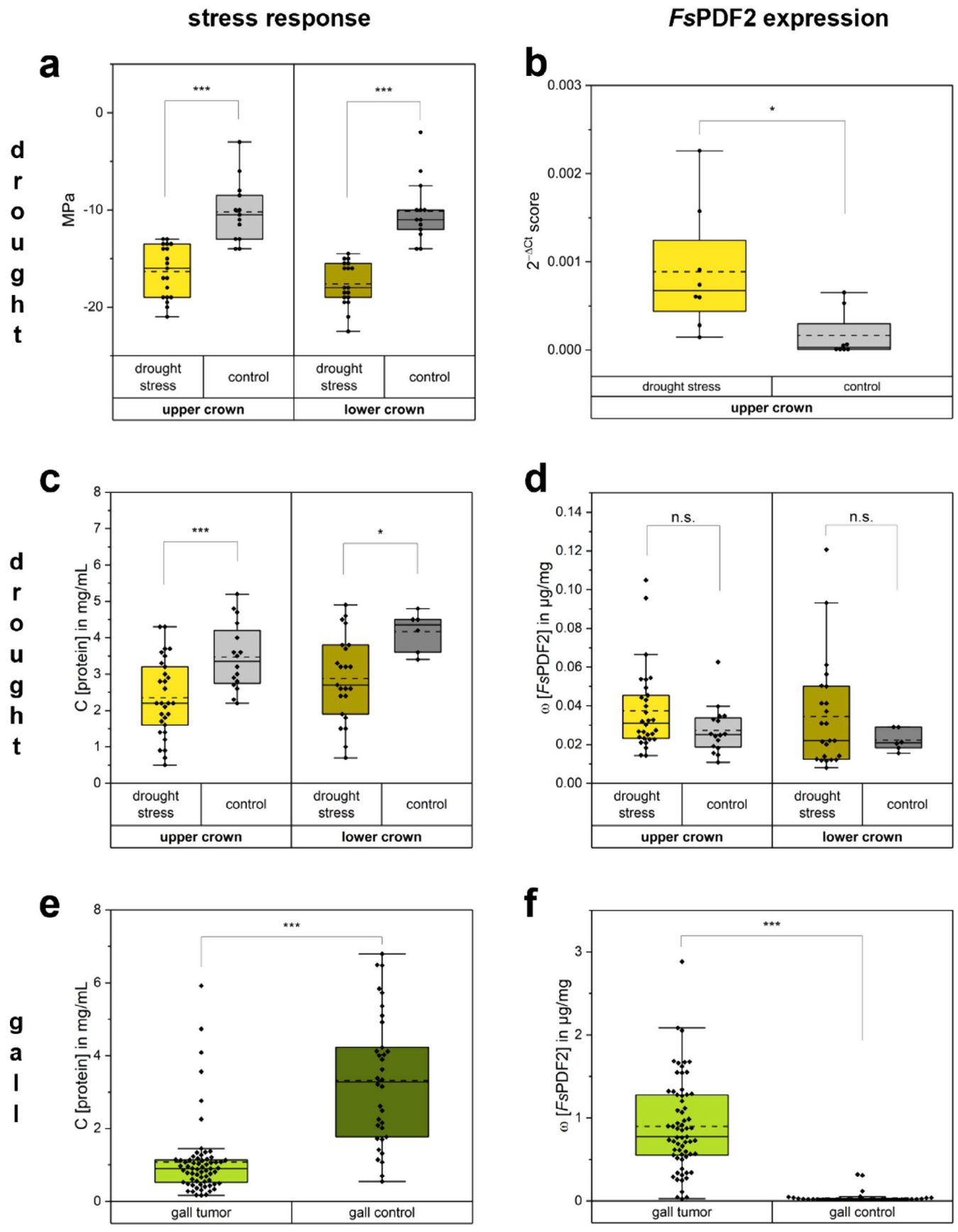

FIGURE 5 | Legend on next page.

FIGURE 5 | *Fs*PDF2 in leaf extracts of stressed beech trees. (a–d) Experiments for *Fs*PDF2 quantification in beech leaves exposed to drought, harvested after several months of drought in September 2019. Stressed trees grew on sandy soil in a dry forest area; control trees were at a lake nearby. (a) Water potential of drought-exposed trees in Britz (drought stress $n = 19$; control $n = 13$). (b) Expression data of *Fs*PDF2 via qPCR of drought-exposed trees in the upper crown of Beerenbusch samples ($n = 8$). c/d Comparison of protein content (c) and defensin content (d) between the upper and lower crown from both locations (number of replicates: Upper crown, drought stress $n = 30$, control $n = 16$; lower crown drought stress $n = 23$, control $n = 6$). e/f Comparison of protein content (e) and defensin content (f) of sample material from *F. sylvatica* leaf gall tumours ($n = 65$) and the surrounding healthy leaf tissue ($n = 34$). One-way ANOVA significance tests at 0.05 (*) and 0.001 (***) were performed.

represent essential components of plant immune defence (dos Santos-Silva et al. 2020; Srivastava et al. 2021). Understanding the AMPs functions and improvement of methods of detection and quantification of these small proteins has become increasingly important in recent years (Bakare et al. 2022). In particular, early diagnostics of forest trees and crop species diseases is a promising area of application of the AMP quantification methods for the future of forestry and agriculture. In an ever more rapidly changing environment, there is no longer time to observe developments only empirically or phenotypically (Bakare et al. 2022; Nosenko et al. 2021).

Molecular monitoring of the state of the plant immune system will make it possible to detect climate-related damage caused by new or increased pressure of native biotic and abiotic stressors more quickly and to initiate silvicultural measures before entire forests or agricultural fields die. In this context, beech, Central Europe's dominant broadleaved tree species, is particularly under pressure (Geßler et al. 2007). Therefore, we have chosen *Fagus sylvatica* to demonstrate the usefulness of AMPs in the early diagnosis of plant damage of economically very important tree species (Bolte et al. 2007). We discovered the most abundant defensin of *F. sylvatica* (*Fs*PDF2) in herbivory stress by genome and transcriptome analysis and investigated its expression in stress response.

Protein-level analyses via ELISA offer a higher diagnostic value in the context of stress physiology compared to transcriptomic methods such as qPCR, which are highly sensitive but often lack predictive power for protein abundance (Guerrero-Sánchez et al. 2021), especially when mRNA-protein correlations are poor. Western blotting and immunohistochemistry were excluded due to a lack of high throughput and accurate quantification capabilities. For robust analyte detection in ELISA, highly specific antibodies are needed.

Antibodies are one of the most important biotechnological tools for measuring and quantifying proteins, e.g., for diagnostic purposes (Aydin 2015). However, depending on the way of their generation, the quality of antibodies differs dramatically (Baker 2015). In particular, polyclonal antibodies exhibit limited reproducibility, batch-to-batch variability, and cross-reactivity, and are not sustainable due to the limited amount obtained from a single source (Andrew and Andreas 2015; Goodman 2018). Until now, only polyclonal antibodies produced in rabbits have been described to detect plant defensins, which could be used in immunoblots (Gao et al. 2000; Jha and Chattoo 2009; Van Der Weerden et al. 2008). Even monoclonal antibodies derived by hybridoma technique could result in non-monospecific antibodies (Bradbury et al. 2018). However, recombinant antibodies offer the best-defined detection reagents as they are always free of contaminating IgG species and defined by their primary structure, assuring unlimited future reproducibility (Ayoubi et al. 2023; Dübel 2024). Therefore, we used in vitro antibody generation by phage display, which allows animal-free generation of sequence-defined recombinant antibodies (Al-Halabi et al. 2013; Colwill et al. 2011; Fuchs et al. 2014; Kuhn et al. 2017). Our antibodies offer high sensitivity (EC50 of 8 nmol), a high specificity for FsPDF2 in beech, reproducibility, and are suitable for diagnostic applications in crude plant extract. However, the first requirement for successful antibody generation is the production of correctly folded antigen in sufficient quantities. For this purpose, we used the baculovirus-free high-five insect cell culture system (Korn et al. 2020), which provided sufficient amounts of highly stable *Fs*PDF2. The recombinant defensin also served for antibody characterisation and *Fs*PDF2 quantification (Figure S2). With this insect cell system, we have demonstrated another possibility for practitioners that could increase the probability that AMPs will be folded correctly if other systems have failed.

Generating a highly specific and sensitive test system for small AMP molecules in crude plant extracts requires two antibodies binding to two distinct and non-overlapping epitopes. This task was challenging for plant defensin *Fs*PDF2 due to the small protein size (5 kDa) and very compact structure. Globular defensins have a diameter of about 24–32 Å, which roughly corresponds to the binding surface of an antibody paratope of about 7–8 amino acids. Since the available epitopes are consequently very limited, the naive human antibody library HAL9/10 with their high diversity of different antibody fragments showed its strength. The HAL9/10 libraries are not limited by the restrictions of the immune system (Kügler et al. 2015), which is an advantage compared to the hybridoma technology using immunised mice. The naïve HAL9/10 libraries showed already their capabilities in deriving high specific monoclonal antibodies against e.g., *Listeria monocytogenes* (Moreira et al. 2022) and *Legionella spec*. (Kuhn et al. 2017) for diagnostic purposes and also antibodies against SARS-CoV-2 (Bertoglio et al. 2021), black widow toxin (Ruschig et al. 2024) and interleukin 5 (Langreder et al. 2023) for therapeutic purposes.

As the in silico model predicts, the antibodies PHE148-H1 and PHE183-B12 can bind simultaneously to the small *Fs*PDF2 and cover a major part of the antigen. This allowed for specific detection of *Fs*PDF2 in crude or complex plant extracts in an ELISA system, which was first demonstrated by recombinant overexpression of *Fs*PDF2 in *N. benthamiana* leaves. As a negative control, *N. benthamiana* extract expressing a non-related protein was used. The control did not show signals in the normal measurement range up to 10 µg/mL extract concentration in the ELISA. Therefore, the ELISA result could be attributed

to specific binding of the antibody to *Fs*PDF2. We were able to detect *Fs*PDF2 – tagged and untagged – expressed in different expression systems, purified and in crude plant extract. The specific antibody–antigen interaction was verified by MS analysis after co-immunoprecipitation, allowing the identification of native *Fs*PDF2 from crude plant extract for PHE148-H1 and recombinant *Fs*PDF2 for both antibodies. Although the EC_{50} values of PHE148-H1 and PHE183-B12 in ELISA are in the same range, PHE148-H1 showed a better performance in capturing native *Fs*PDF2 out of crude extract. Antibody pairs that perform differently in reversed order in sandwich ELISA have been observed before (Al-Halabi et al. 2013). Therefore, the ELISA signal results from specific binding of the antibodies to *Fs*PDF2. Additionally, AlphaFold 3 gives a rational model of how the antibodies bind to the antigen.

A weak cross-reaction was also observed in the *N. benthamiana* negative control extract used in high protein concentrations. As the structure of defensins has remained highly conserved during evolution (Parisi et al. 2019), it is possible that the antibodies can bind closely related defensins from tobacco. However, this cross-reaction does not play a role in the diagnostic ELISA as the LC–MS/MS data show that the antibodies are highly specific for *Fs*PDF2 in crude beech extract. Therefore, no off-target binding was observed in the homologous *Fagus sylvatica* system, validating the robustness of the ELISA in native conditions. Contrariwise, research can even take advantage of the high evolutionary conservation of defensin domains across plant taxa. These concentrations exceed the ELISA's operating range because it may allow the usage of antibodies generated against homologous defensins in closely related species without the generation of new ones.

However, the leaves of most trees contain significant amounts of tannins and other interfering phytochemicals that interfere with protein extraction and ELISA (Hemingway and Karchesy 1989). We added PVP during extraction to adsorb the protein-denaturing tannins to reduce the interference from plant secondary metabolites. In addition, adding PVP to block and antibody solutions improved the signal-to-noise ratio.

With this immunological detection system, we were able to measure endogenous defensin levels of *Fs*PDF2 in beech tissue extract. While unstressed leaves had just no or a low basal *Fs*PDF2 expression, beech embryos had a much higher amount of defensins. This confirms the hypothesis that seeds have a high content of defensins to protect themselves and, in particular, the embryo from herbivores and pathogens. For example, in *Raphanus sativus*, defensins make 0.5% of the total seed protein (Thomma et al. 2002). Therefore, the result demonstrates that our sandwich ELISA with specific monoclonal antibodies allows rapid and robust defensin quantification in crude beech extract.

So far, changes in defensin regulation to quantify stress response were only detected using transcriptomic data, e.g., for *Dhn8* from soybean, which showed a 10-fold upregulation of transcript levels under drought stress (Maitra and Cushman 1994), or with a 40- and 8-fold upregulation in inner and outer gall midge tumour tissue of oak (Martinson et al. 2020), respectively. In our ELISA study, drought stress elicited no significant *Fs*PDF2 response, which is in contrast to the transcript data with 24 times upregulation. This can be caused by the transport of the apoplastic-located defensins from leaves to other organs, a faster usage under stress, or a poor correlation between transcription and translation caused by a lack of resources under stress. Such a poor correlation between the transcript and protein level was recently observed for a lot of proteins in *Quercus ilex* under drought stress (Guerrero-Sánchez et al. 2021). The poor correlation between transcriptomic and proteomic data, due to potential apoplastic transportation effects, shows the importance of stress monitoring on protein level, which highlights ELISA as a robust, fast and sensitive methodology. Also, when plant secondary metabolites interfere with molecular diagnostics, the ELISA used here was not substantially impaired (see also Figure S7).

However, a strong stress response in beech galls in response to gall midge larvae was demonstrated. Gall midges lay their eggs in leaves, which develop into larvae that secrete metabolites stimulating plants to form conspicuous galls (Pilichowski and Giertych 2021). Since gall midges are pests to beech, it is reasonable to assume that defensins are among the plant proteins involved in the defence against the invader. We were able to detect elevated *Fs*PDF2 levels distinctly in the gall and not in the surrounding tissue, showing that the leaves respond very specifically and locally to the presence of the larva. The tested gall midge tumours had a *Fs*PDF proportion of around 0.9‰ of total protein mass.

5 | Conclusions

Our strategy could be extended by practitioners in the future to other AMPs and other types of stress. This study establishes a robust framework for generating monoclonal antibodies against small AMPs, using FsPDF2 as a structurally representative model. The antibody selection process was tailored to the compact, cysteine-rich structure typical of defensins, with optimized panning conditions that ensured correct antigen folding and epitope accessibility. In vitro antibody generation by adapted phage display panning strategies in combination with in silico structure prediction presented here can serve as a biotechnological template to make other small and compact AMPs detectable. These methodological features are inherently generalisable to other AMPs with similar biophysical constraints, particularly within the defensin family, which shares conserved tertiary motifs (Parisi et al. 2019). The antigen design for small proteins can be adapted to the characteristics of other AMPs. This approach offers an additional chance for AMP research on the protein level.

To evaluate assay robustness, we included a range of sample types encompassing multiple tissue sources (leaves, embryos), biotic and abiotic stress conditions (gall midge infestation, drought) and distinct ecological sites. Of particular interest would be the use as a diagnostic tool for the detection of other abiotic and biotic stress conditions in a field application with rapid on-site tests based on lateral flow assays. Not all stressors are as easy to recognize as gall midges, so countermeasures against other stressors could be initiated at an early stage, long before visible symptoms appear. With AMP quantification via

ELISA, a deeper analysis of stress in trees is now possible, especially since transcript and protein levels often correlate poorly, and a large number of secondary metabolites make RNA-based detection methods difficult. Identification of stress in *F. sylvatica* by defensins in native samples would be a powerful tool for forest monitoring that meets the growing challenges of climate change.

We hope that our study will stimulate further research on AMPs from plants, but also from animals. AMPs will continue to gain importance, especially regarding their medicinal benefits for plants, animals and humans.

Author Contributions

R.H., H.R., J.-P.S., S.D., M.H., J.S. and D.K. planned/designed the project and acquired funding. D.K., T.N., M.H.-U., A.S., S.K., J.B.W. and R.H. performed plant experiments and harvested plant samples. T.N. performed in silico studies and DNA/RNA sequencing. K.D.O. performed in silico structure modeling. A.S. and B.H. performed qPCR analyses. P.A.H., N.L., T.L., J.K., S.P., D.S., M.S. and D.K. produced the recombinant defensins. P.A.H., M.B., V.P. and D.M. produced and quality checked the antibodies. P.A.H. and S.P. performed the antibody phage display. P.A.H., S.K., N.G., N.L., T.L., A.P. and D.K. optimized and performed ELISA. S.E., M.K. and S.K. performed MS/MS experiments. All authors analysed and discussed the results. P.A.H. and D.K. were primarily involved in drafting the manuscript, while K.D.O., S.E., M.K., S.K. and T.N. wrote specific chapters. P.A.H., K.D.O., T.N., M.K. and D.K. produced figures and tables. R.H., J.-P.S., H.R., S.D., M.H., M.S. and K.D.O. critically read the manuscript and improved the text; all authors finalised it. R.H., D.K. and P.A.H. coordinated the work.

Acknowledgements

We thank Jette Duschka, Viola Fühner, Benedikt Gierling, Dianne Gnann, Sarah Mara Stella Köllner, Philipp Körsgen, Noah Kurzawa and Hanna Willenbockel for their high commitment, providing figure templates, proofreading and excellent technical work in our lab. Figure 1 was created with BioRender.com. Calculation curves were computed with OriginPro, Version 2024, OriginLab Corporation, Northampton, MA, USA. Sequences were analysed with Geneious version 2024.0 created by Biomatters. Available from https://www.geneious.com. Open Access funding enabled and organized by Projekt DEAL.

Conflicts of Interest

The authors declare no conflicts of interest.

Data Availability Statement

The data that support the findings of this study are available on request from the corresponding author. The data are not publicly available due to privacy or ethical restrictions.

References

Abramson, J., J. Adler, J. Dunger, et al. 2024. "Accurate Structure Prediction of Biomolecular Interactions With AlphaFold 3." *Nature* 630: 493–500.

Al-Halabi, L., A. Balck, M. Michalzik, et al. 2013. "Recombinant Antibody Fragments Allow Repeated Measurements of C-Reactive Protein With a Quartz Crystal Microbalance Immunosensor." *MAbs* 5: 140–149.

Andrew, B., and P. Andreas. 2015. "Reproducibility: Standardize Antibodies Used in Research." *Nature* 518: 27–29.

Andrews, S. 2010. *FastQC: A Quality Control Tool for High Throughput Sequence Data*. Babraham Bioinformatics. https://www.bioinformatics.babraham.ac.uk/projects/fastqc/.

Arputharaj, A. J. 2017. "Role of the Defensin-Like Protein Gene Family in Plant Reproductive Isolation and Disease Resistance in *Arabidopsis thaliana*." PhD.

Aydin, S. 2015. "A Short History, Principles, and Types of ELISA, and Our Laboratory Experience With Peptide/Protein Analyses Using ELISA." *Peptides* 72: 4–15.

Ayoubi, R., J. Ryan, M. S. Biddle, et al. 2023. "Scaling of an Antibody Validation Procedure Enables Quantification of Antibody Performance in Major Research Applications." *eLife* 12: RP91645.

Bakare, O. O., A. Gokul, A. O. Fadaka, et al. 2022. "Plant Antimicrobial Peptides (PAMPs): Features, Applications, Production, Expression and Challenges." *Molecules* 27: 3703.

Baker, M. 2015. "Blame It on the Antibodies." *Nature* 521, no. 7552: 274–276.

Bertoglio, F., D. Meier, N. Langreder, et al. 2021. "SARS-CoV-2 Neutralizing Human Recombinant Antibodies Selected From Pre-Pandemic Healthy Donors Binding at RBD-ACE2 Interface." *Nature Communications* 12: 1–15.

Bleckmann, M., M. H. Y. Fritz, S. Bhuju, et al. 2015. "Genomic Analysis and Isolation of RNA Polymerase II Dependent Promoters From *Spodoptera frugiperda*." *PLoS One* 10: 1–16.

Bolger, A. M., M. Lohse, and B. Usadel. 2014. "Trimmomatic: A Flexible Trimmer for Illumina Sequence Data." *Bioinformatics* 30: 2114–2120. https://doi.org/10.1093/bioinformatics/btu170.

Bolte, A., T. Czajkowski, and T. Kompa. 2007. "The North-Eastern Distribution Range of European Beech—A Review." *Forestry* 80: 413–429.

Bradbury, A. R. M., N. D. Trinklein, H. Thie, et al. 2018. "When Monoclonal Antibodies Are Not Monospecific: Hybridomas Frequently Express Additional Functional Variable Regions." *MAbs* 10: 539–546.

Breitling, F., S. Diibel, T. Seehaus, I. Klewinghaus, and M. Little. 1991. "A Surface Expression Vector for Antibody Screening (Phage Gene III; Fusion Protein; Phagemid; Library; Recombinant DNA)." *Gene* 104: 147–353.

Brogden, K. A. 2005. "Antimicrobial Peptides: Pore Formers or Metabolic Inhibitors in Bacteria?" *Nature Reviews. Microbiology* 3: 238–250.

Camacho, C., G. Coulouris, V. Avagyan, et al. 2009. "BLAST+: Architecture and Applications." *BMC Bioinformatics* 10: 1–9.

Colwill, K., S. Gräslund, H. Persson, et al. 2011. "A Roadmap to Generate Renewable Protein Binders to the Human Proteome." *Nature Methods* 8: 551–561.

De Beer, A., and M. A. Vivier. 2011. "Four Plant Defensins From an Indigenous South African Brassicaceae Species Display Divergent Activities Against Two Test Pathogens Despite High Sequence Similarity in the Encoding Genes." *BMC Research Notes* 4: 459.

De Coninck, B., B. P. A. Cammue, and K. Thevissen. 2013. "Modes of Antifungal Action and in Planta Functions of Plant Defensins and Defensin-Like Peptides." *Fungal Biology Reviews* 26: 109–120.

de Oliveira Carvalho, A., and V. Moreira Gomes. 2012. "Plant Defensins and Defensin-Like Peptides—Biological Activities and Biotechnological Applications." *Current Pharmaceutical Design* 17: 4270–4293.

Dobin, A., C. A. Davis, F. Schlesinger et al. 2013. "STAR: Ultrafast Universal RNA-seq Aligner." *Bioinformatics* 29: 15–21. https://doi.org/10.1093/bioinformatics/bts635.

dos Santos-Silva, C. A., L. Zupin, M. Oliveira-Lima, et al. 2020. "Plant Antimicrobial Peptides: State of the Art, In Silico Prediction and Perspectives in the Omics Era." *Bioinformatics and Biology Insights* 14: 1177932220952739.

Drozdetskiy, A., C. Cole, J. Procter, and G. J. Barton. 2015. "JPred4: A Protein Secondary Structure Prediction Server." *Nucleic Acids Research* 43: W389–W394.

Dübel, S. 2024. "Can Antibodies Be "Vegan"? A Guide Through the Maze of Today's Antibody Generation Methods." *MAbs* 16: 2343499.

Dyderski, M. K., S. Paź, L. E. Frelich, and A. M. Jagodziński. 2018. "How Much Does Climate Change Threaten European Forest Tree Species Distributions?" *Global Change Biology* 24: 1150–1163.

Fuchs, M., S. Kämpfer, S. Helmsing, et al. 2014. "Novel Human Recombinant Antibodies Against *Mycobacterium tuberculosis* Antigen 85B." *BMC Biotechnology* 14: 1–16.

Fuchs, S., M. Kucklick, E. Lehmann, et al. 2021. "Towards the Characterization of the Hidden World of Small Proteins in *Staphylococcus aureus*, a Proteogenomics Approach." *PLoS Genetics* 17: e1009585.

Gao, A. G., S. M. Hakimi, C. A. Mittanck, et al. 2000. "Fungal Pathogen Protection in Potato by Expression of a Plant Defensin Peptide." *Nature Biotechnology* 18: 1307–1310.

Geßler, A., C. Keitel, J. Kreuzwieser, R. Matyssek, W. Seiler, and H. Rennenberg. 2007. "Potential Risks for European Beech (*Fagus sylvatica* L.) in a Changing Climate." *Trees-Structure and Function* 21: 1–11.

Goodman, S. L. 2018. "The Antibody Horror Show: An Introductory Guide for the Perplexed." *New Biotechnology* 45: 9–13.

Guerrero-Sánchez, V. M., M. Á. Castillejo, C. López-Hidalgo, A. M. M. Alconada, J. V. Jorrín-Novo, and M. D. Rey. 2021. "Changes in the Transcript and Protein Profiles of *Quercus ilex* Seedlings in Response to Drought Stress." *Journal of Proteomics* 243: 104263.

Hamisch, D., D. Randewig, S. Schliesky, et al. 2012. "Impact of SO2 on *Arabidopsis thaliana* Transcriptome in Wildtype and Sulfite Oxidase Knockout Plants Analyzed by RNA Deep Sequencing." *New Phytologist* 196: 1074–1085.

Heine, P. A., M. Ruschig, N. Langreder, et al. 2023. "Antibody Selection in Solution Using Magnetic Beads." In *Phage Display: Methods and Protocols*, 261–274. Springer US.

Hemingway, R. W., and J. J. Karchesy. 1989. "Chemistry and Significance of Condensed Tannins." Proceedings of the FIRST North American Tannin Conference: Plenum Press, New York.

Hughes, C. S., S. Foehr, D. A. Garfield, E. E. Furlong, L. M. Steinmetz, and J. Krijgsveld. 2014. "Ultrasensitive Proteome Analysis Using Paramagnetic Bead Technology." *Molecular Systems Biology* 10: 757.

Järvå, M., F. T. Lay, M. D. Hulett, and M. Kvansakul. 2017. "Structure of the Defensin NsD7 in Complex With PIP2 Reveals That Defensin: Lipid Oligomer Topologies Are Dependent on Lipid Type." *FEBS Letters* 591: 2482–2490.

Jha, S., and B. B. Chattoo. 2009. "Transgene Stacking and Coordinated Expression of Plant Defensins Confer Fungal Resistance in Rice." *Rice* 2: 143–154.

Karimi, M., D. Inzé, and A. Depicker. 2002. "GATEWAY Vectors for Agrobacterium-Mediated Plant." *Trends in Plant Science* 7: 193–195.

Kaufholdt, D., C. Gehl, M. Geisler, et al. 2013. "Visualization and Quantification of Protein Interactions in the Biosynthetic Pathway of Molybdenum Cofactor in *Arabidopsis thaliana*." *Journal of Experimental Botany* 64: 2005–2016.

Kõressaar, T., M. Lepamets, L. Kaplinski, K. Raime, R. Andreson, and M. Remm. 2018. "Primer3-Masker: Integrating Masking of Template Sequence With Primer Design Software." *Bioinformatics* 34: 1937–1938.

Korn, J., D. Schäckermann, T. Kirmann, et al. 2020. "Baculovirus-Free Insect Cell Expression System for High Yield Antibody and Antigen Production." *Scientific Reports* 10: 1–10.

Kügler, J., S. Wilke, D. Meier, et al. 2015. "Generation and Analysis of the Improved Human HAL9/10 Antibody Phage Display Libraries." *BMC Biotechnology* 15: 1–15.

Kuhn, P., S. Thiem, M. Steinert, et al. 2017. "Human Anti-Lipopolysaccharid (LPS) Antibodies Against Legionella With High Species Specificity." *Human Antibodies* 26: 29–38.

Lacerda, A. F., É. A. R. Vasconcelos, P. B. Pelegrini, and M. F. Grossi de Sa. 2014. "Antifungal Defensins and Their Role in Plant Defense." *Frontiers in Microbiology* 5: 1–10.

Langreder, N., D. Schäckermann, D. Meier, et al. 2023. "Development of an Inhibiting Antibody Against Equine Interleukin 5 to Treat Insect Bite Hypersensitivity of Horses." *Scientific Reports* 13: 4029.

Lawrence, M., W. Huber, H. Pagès, et al. 2013. "Software for Computing and Annotating Genomic Ranges." *PLoS Computational Biology* 9: 1–10.

Lay, F., and M. Anderson. 2005. "Defensins—Components of the Innate Immune System in Plants." *Current Protein & Peptide Science* 6: 85–101.

Lazzaro, B. P., M. Zasloff, and J. Rolff. 2020. "Antimicrobial Peptides: Application Informed by Evolution." *Science* 368: eaau5480.

Liao, Y., G. K. Smyth, and W. Shi. 2014. "FeatureCounts: An Efficient General Purpose Program for Assigning Sequence Reads to Genomic Features." *Bioinformatics* 30: 923–930. https://doi.org/10.1093/bioinformatics/btt656.

Liu, X., H. Zhang, H. Jiao, et al. 2017. "Expansion and Evolutionary Patterns of Cysteine-Rich Peptides in Plants." *BMC Genomics* 18: 1–14.

Livak, K. J., and T. D. Schmittgen. 2001. "Analysis of Relative Gene Expression Data Using Real-Time Quantitative PCR and the 2−ΔΔCT Method." *Methods* 25: 402–408.

Lobo, D. S., I. B. Pereira, L. Fragel-Madeira, et al. 2007. "Antifungal *Pisum sativum* Defensin 1 Interacts With *Neurospora crassa* Cyclin F Related to the Cell Cycle." *Biochemistry* 46: 987–996.

Magalhães, P. J., J. S. Vieira, L. M. Gonçalves, J. G. Pacheco, L. F. Guido, and A. A. Barros. 2010. "Isolation of Phenolic Compounds From Hop Extracts Using Polyvinylpolypyrrolidone: Characterization by High-Performance Liquid Chromatography-Diode Array Detection-Electrospray Tandem Mass Spectrometry." *Journal of Chromatography. A* 1217: 3258–3268.

Maitra, N., and J. C. Cushman. 1994. "Isolation and Characterization of a Drought-Induced Soybean cDNA Encoding a D95 Family Late-Embryogenesis-Abundant Protein." *Plant Physiology* 106: 805–806.

Martinson, E., J. Werren, and S. Egan. 2020. "Tissue-Specific Gene Expression Shows Cynipid Wasps Repurpose Host Gene Networks to Create Complex and Novel Parasite-Specific Organs on Oaks." Authorea Preprints. 1–14.

Mateus, A., J. Bobonis, N. Kurzawa, et al. 2018. "Thermal Proteome Profiling in Bacteria: Probing Protein State In Vivo." *Molecular Systems Biology* 14: e8242.

Méndez, E., A. Rocher, M. Calero, T. Girbés, L. Citores, and F. Soriano. 1996. "Primary Structure of ω-Hordothionin, a Member of a Novel Family of Thionins From Barley Endosperm, and Its Inhibition of Protein Synthesis in Eukaryotic and Prokaryotic Cell-Free Systems." *European Journal of Biochemistry* 239: 67–73.

Mirdita, M., K. Schütze, Y. Moriwaki, L. Heo, S. Ovchinnikov, and M. Steinegger. 2022. "ColabFold: Making Protein Folding Accessible to All." *Nature Methods* 19: 679–682.

Mirouze, M., J. Sels, O. Richard, et al. 2006. "A Putative Novel Role for Plant Defensins: A Defensin From the Zinc Hyper-Accumulating Plant, Arabidopsis Halleri, Confers Zinc Tolerance." *Plant Journal* 47: 329–342.

Mishra, B., D. K. Gupta, M. Pfenninger, et al. 2018. "A Reference Genome of the European Beech (*Fagus sylvatica* L.)." *GigaScience* 7: giy063.

Moreira, G. M. S. G., S. Gronow, S. Dübel, et al. 2022. "Phage Display-Derived Monoclonal Antibodies Against Internalins A and B Allow Specific Detection of *Listeria monocytogenes*." *Frontiers in Public Health* 10: 712657.

Nielsen, H. 2017. "Predicting Secretory Proteins With SignalP." *Protein Function Prediction: Methods and Protocols* 1611: 59–73.

Nosenko, T., M. Hanke-Uhe, P. A. Heine, et al. 2021. "Plant Defense Proteins as Potential Markers for Early Detection of Forest Damage and Diseases." *Frontiers in Forests and Global Change* 4: 1–5.

Parisi, K., T. Ma, P. Quimbar, N. L. Van Der Weerden, and M. R. Bleackley. 2019. "The Evolution, Function and Mechanisms of Action for Plant Defensins." *Seminars in Cell & Developmental Biology* 88: 107–118.

Perez-Riverol, Y., C. Bandla, D. J. Kundu, et al. 2025. "The PRIDE Database at 20 Years: 2025 Update." *Nucleic Acids Research* 53: D543–D553.

Pettersen, E. F., T. D. Goddard, C. C. Huang, et al. 2021. "UCSF ChimeraX: Structure Visualization for Researchers, Educators, and Developers." *Protein Science* 30: 70–82.

Pilichowski, S., and M. J. Giertych. 2021. "Two Galling Insects (*Hartigiola annulipes* and *Mikiola fagi*), One Host Plant (*Fagus sylvatica*)—Differences Between Leaf and Gall Chemical Composition." *Baltic Forestry* 26: 1–11.

Robinson, J. T., H. Thorvaldsdóttir, W. Winckler, et al. 2011. "Integrative Genomics Viewer." *Nature Biotechnology* 29, no. 1: 24–26.

Rondot, S., J. Koch, F. Breitling, and S. Dübel. 2001. "A Helper Phage to Improve Single-Chain Antibody Presentation in Phage Display." *Nature Biotechnology* 19: 75–78.

Ruschig, M., J. Nerlich, M. Becker, et al. 2024. "Human Antibodies Neutralizing the Alpha-Latrotoxin of the European Black Widow." *Frontiers in Immunology* 15: 1407398.

Scholander, P. F., H. T. Hammel, E. D. Bradstreet, and E. A. Hemmingsen. 1965. "Sap Pressure in Vascular Plants Negative Hydrostatic Pressure Can Be Measured in Plants." Sap Pressure in Vascular Plants Published by: American Association for the Advancement of Science Linked References Are Available on JSTOR for This Article (1979). *Science* 148: 339–346.

Silverstein, K. A. T., M. A. Graham, T. D. Paape, and K. A. Vandenbosch. 2005. "Genome Organization of More Than 300 Defensin-Like Genes in Arabidopsis." *Plant Physiology* 138: 600–610.

Soltes, G., M. Hust, K. K. Y. Ng, et al. 2007. "On the Influence of Vector Design on Antibody Phage Display." *Journal of Biotechnology* 127: 626–637.

Spelbrink, R. G., N. Dilmac, A. Allen, T. J. Smith, D. M. Shah, and G. H. Hockerman. 2004. "Differential Antifungal and Calcium Channel-Blocking Activity Among Structurally Related Plant Defensins." *Plant Physiology* 135: 2055–2067.

Srivastava, S., K. Dashora, K. L. Ameta, et al. 2021. "Cysteine-Rich Antimicrobial Peptides From Plants: The Future of Antimicrobial Therapy." *Phytotherapy Research* 35: 256–277.

Stanke, M., M. Diekhans, R. Baertsch, and D. Haussler. 2008. "Using Native and Syntenically Mapped cDNA Alignments to Improve De Novo Gene Finding." *Bioinformatics* 24: 637–644.

Stenlid, J., and J. Oliva. 2016. "Phenotypic Interactions Between Tree Hosts and Invasive Forest Pathogens in the Light of Globalization and Climate Change." *Philosophical Transactions of the Royal Society, B: Biological Sciences* 371: 20150455.

Thomma, B. P. H. J., B. P. A. Cammue, and K. Thevissen. 2002. "Plant Defensins." *Planta* 216: 193–202.

Tomisawa, S., C. Abe, M. Kamiya, et al. 2013. "A New Approach to Detect Small Peptides Clearly and Sensitively by Western Blotting Using a Vacuum-Assisted Detection Method." *Biophysics* 9: 79–83.

Uotila, M., E. Ruoslahti, and E. Engvall. 1981. "Two-Site Sandwich Enzyme Immunoassay With Monoclonal Antibodies to Human Alpha-Fetoprotein." *Journal of Immunological Methods* 42: 11–15.

van der Weerden, N. L., and M. A. Anderson. 2013. "Plant Defensins: Common Fold, Multiple Functions." *Fungal Biology Reviews* 26: 121–131.

Van Der Weerden, N. L., F. T. Lay, and M. A. Anderson. 2008. "The Plant Defensin, NaD1, Enters the Cytoplasm of *Fusarium oxysporum* Hyphae." *Journal of Biological Chemistry* 283: 14445–14452.

Weber, J. N., D. Kaufholdt, R. Minner-Meinen, et al. 2021. "Impact of Wildfires on SO2 Detoxification Mechanisms in Leaves of Oak and Beech Trees." *Environmental Pollution* 272: 116389.

Wenzel, E. V., M. Bosnak, R. Tierney, et al. 2020. "Human Antibodies Neutralizing Diphtheria Toxin In Vitro and In Vivo." *Scientific Reports* 10: 1–21.

Xu, J., and Y. Zhang. 2010. "How Significant Is a Protein Structure Similarity With TM-Score = 0.5?" *Bioinformatics* 26: 889–895.

Yount, N. Y., and M. R. Yeaman. 2004. "Multidimensional Signatures in Antimicrobial Peptides." *Proceedings of the National Academy of Sciences of the United States of America* 101: 7363–7368.

Yusypovych, Y. M. 2016. "Defensin-Like Sequences in the Genomes of Fagales Species." *Scientific Bulletin of NLTU of Ukraine* 26, no. 4: 163–169 (in Ukrainian). 8–11.

Zhang, Y., and J. Skolnick. 2004. "Scoring Function for Automated Assessment of Protein Structure Template Quality." *Proteins: Structure, Function, and Bioinformatics* 57: 702–710.

Supporting Information

Additional supporting information can be found online in the Supporting Information section. **Figure S1:** Amino acid sequence of recombinant *Fs*PDF2. **Figure S2:** Initial ColabFold model of FsPDF2 in complex with PHE148-H1 and PHE183-B12. **Figure S3:** Results of Titration ELISA revealing the stability of recombinant FsPDF2 from High Five insect cells at varied temperatures. **Figure S4:** Binding of the HAL10 scFv fragments to FsPSF2. **Figure S5:** Influence of tannins in the ELISA. **Figure S6:** ELISA with different blocking agents. **Figure S7:** Detection of recombinant FsPDF2 in crude plant extract. **Figure S8:** Drought stress demonstration. **Figure S9:** *Fs*PDF2 quantification in beech leaves exposed to drought. **Data S1:** Alignments of plant defensin amino acid sequences used in this study for constructing the defensin profiles for Augustus-PPX. **Data S2:** Amino acid sequences of the Fagus sylvatica defensin genes predicted using Augustus-PPX. **Table S1:** Genomic coordinates and expression information for the predicted Fagus sylvatica defensin genes. **Table S2:** List of synthesised gene sequences and used primers. **Table S3:** Co-immunoprecipitation (CoIP) and LC–MS/MS analysis for specificity validation of PHE148-H1 and PHE183-B12.